The American Journal of Pathology, Vol. 184, No. 6, June 2014

ELSEVIER

The American Journal of
PATHOLOGY
ajp.amjpathol.org

CARDIOVASCULAR, PULMONARY, AND RENAL PATHOLOGY

# Endothelin-1 Activation of the Endothelin B Receptor Modulates Pulmonary Endothelial CX3CL1 and Contributes to Pulmonary Angiogenesis in Experimental Hepatopulmonary Syndrome

Junlan Zhang, Wenli Yang, Bingqian Hu, Wei Wu, and Michael B. Fallon

*From the Division of Gastroenterology, Hepatology, and Nutrition, the Department of Internal Medicine, The University of Texas Health Science Center at Houston, Houston, Texas*

Accepted for publication February 11, 2014.

Address correspondence to Michael B. Fallon, M.D., Division of Gastroenterology, Hepatology, and Nutrition, Department of Internal Medicine, The University of Texas Health Science Center at Houston, 6431 Fannin St, Medical School Building 4.234, Houston, TX 77030-1501. E-mail: michael.b.fallon@uth.tmc.edu.

Hepatic production and release of endothelin-1 (ET-1) binding to endothelin B ($ET_B$) receptors, overexpressed in the lung microvasculature, is associated with accumulation of pro-angiogenic monocytes and vascular remodeling in experimental hepatopulmonary syndrome (HPS) after common bile duct ligation (CBDL). We have recently found that lung vascular monocyte adhesion and angiogenesis in HPS involve interaction of endothelial C-X3-C motif ligand 1 (CX3CL1) with monocyte CX3C chemokine receptor 1 (CX3CR1), although whether ET-1/$ET_B$ receptor activation influences these events is unknown. Our aim was to define if ET-1/$ET_B$ receptor activation modulates CX3CL1/CX3CR1 signaling and lung angiogenesis in experimental HPS. A selective $ET_B$ receptor antagonist, BQ788, was given for 2 weeks to 1-week CBDL rats. ET-1 (±BQ788) was given to cultured rat pulmonary microvascular endothelial cells overexpressing $ET_B$ receptors. BQ788 treatment significantly decreased lung angiogenesis, monocyte accumulation, and CX3CL1 levels after CBDL. ET-1 treatment significantly induced CX3CL1 production in lung microvascular endothelial cells, which was blocked by inhibitors of $Ca^{2+}$ and mitogen-activated protein kinase (MEK)/ERK pathways. ET-1—induced ERK activation was $Ca^{2+}$ independent. ET-1 administration also increased endothelial tube formation *in vitro*, which was inhibited by BQ788 or by blocking $Ca^{2+}$ and MEK/ERK activation. CX3CR1 neutralizing antibody partially inhibited ET-1 effects on tube formation. These findings identify a novel mechanistic interaction between the ET-1/$ET_B$ receptor axis and CX3CL1/CX3CR1 in mediating pulmonary angiogenesis and vascular monocyte accumulation in experimental HPS. *(Am J Pathol 2014, 184: 1706—1714; http://dx.doi.org/10.1016/j.ajpath.2014.02.027)*

Cirrhosis and portal hypertension result in vascular alterations in several organ systems, which impair the function of these organs.[1,2] The hepatopulmonary syndrome (HPS) is one such complication, in which intrapulmonary vascular abnormalities cause abnormal arterial gas exchange in 5% to 30% of cirrhotic patients.[3—5] The presence of HPS significantly decreases quality of life and increases mortality in those affected.[6] Currently, the pathogenesis of vascular alterations in HPS is incompletely understood, limiting the development of effective medical therapies.

Chronic common bile duct ligation (CBDL) in the rat is an established experimental model of HPS that reproduces the physiological abnormalities of human disease.[7—16] These animals develop pulmonary microvascular dilations and also develop vascular remodeling, which is linked to the accumulation of intravascular monocytes and vascular endothelial growth factor-A (VEGF-A) production.[11,12,17,18] Pulmonary vasodilation results, in large part, from $Ca^{2+}$-dependent and protein kinase B/Akt—independent activation of pulmonary vascular endothelial nitric oxide synthase (eNOS)/NO, by hepatic production and release of endothelin-1 (ET-1) and stimulation of lung vascular endothelin B ($ET_B$) receptors.[9,19] ET-1/$ET_B$ receptor activation also enhances pulmonary vascular

Supported by NIH grant 5DKR01DK056804 (M.B.F.).
Disclosures: None declared.


http://dx.doi.org/10.1016/j.ajpath.2014.02.027

monocyte accumulation,[14] thereby promoting angiogenesis through monocyte VEGF-A production and activation of Akt and ERK. However, how ET-1/$ET_B$ receptor activation modulates monocyte accumulation and whether $ET_B$ receptor activation has direct effects on angiogenesis are unknown.

We have recently found that the chemokine ligand/receptor pair C-X3-C motif ligand 1 (CX3CL1)/CX3C chemokine receptor 1 (CX3CR1) is up-regulated in the pulmonary microvasculature after CBDL and contributes to monocyte accumulation and to angiogenesis after CBDL.[20] Interaction between the membrane-bound form of CX3CL1 with CX3CR1 is unique in the ability to cause firm adhesion between cell types (monocyte-endothelium).[21–24] In addition, the secreted soluble form of CX3CL1, through interaction with the CX3CR1 on endothelial cells, can drive angiogenesis through Akt and ERK activation.[25] However, whether ET-1/$ET_B$ receptor activation after CBDL influences monocyte accumulation or angiogenesis by affecting lung CX3CL1/CX3CR1 expression has not been tested. Therefore, the aims of the present study were to define if the ET-1/$ET_B$ receptor activation modulates the pulmonary CX3CL1/CX3CR1 axis and to determine how it contributes to vascular remodeling in experimental HPS. To do this, we assessed the effects of selective ET receptor inhibition on pulmonary angiogenesis and CX3CL1/CX3CR1 expression *in vivo* and evaluated the effects of exogenous ET-1 on pulmonary microvascular endothelial cell CX3CL1 expression and angiogenesis *in vitro*.

## Materials and Methods

### Animals

Male Sprague-Dawley rats (Charles River, Wilmington, MA), 250 to 300 g, were subjected to CBDL (the common bile duct was doubly ligated and divided) or sham operation (mobilization of the common bile duct without ligation), after i.p. injection of 80/10 mg/kg ketamine/xylazine to achieve anesthesia.[8,14,26] A selective $ET_B$ receptor antagonist, BQ788 ($1 \times 10^{-7}$ mol/day; Calbiochem, San Diego, CA), or saline was given i.v. using a miniosmotic pump (ALZET model 2002; ALZET, Cupertino, CA) placed into the femoral vein for 2 weeks to 1-week CBDL rats, as previously described.[14] All assessments were made at 3 weeks after surgery. Eight animals were used in each group. Portal venous pressure and spleen weight were measured to evaluate the development of portal hypertension. Lung and plasma samples were obtained for further analysis. The study was approved by the University of Texas at Houston Health Science Center Animal Welfare Committee and conformed to NIH guidelines on the use of laboratory animals.

### Arterial Blood Gas Analysis

Arterial blood was drawn from the femoral artery, as previously described,[8,12,14] and analyzed on an ABL80 FLEX blood gas analyzer (Radiometer America, Westlake, OH). The alveolar-arterial oxygen gradient ($AaPO_2$) was calculated as follows:

$$150 - (PaCO_2/0.8) - PaO_2. \quad (1)$$

### Immunofluorescence and IHC Data

Sections (5 μm thick) of 4% paraformaldehyde, paraffin-fixed lung and liver tissues were blocked and incubated with primary antibodies. For immunofluorescent staining of ED1 (a monocyte marker; Serotec, Raleigh, NC) and factor VIII (FVIII; Cell Marque, Austin, TX), Texas Red and fluorescein secondary antibodies (Vector Laboratories, Burlingame, CA) and mounting medium with DAPI (Vector Laboratories) were used. For immunostaining of ED1, ED2 (tissue resident macrophage marker; Serotec), CD3 (T-cell marker; Abcam, Cambridge, MA), and CD45R (B-cell marker; eBioscience, San Diego, CA), biotinylated secondary antibodies were used. After incubation with streptavidin–biotin–horseradish peroxidase (Vector Laboratories), peroxidase activity was detected with the DAB Peroxidase Substrate Kit (Vector Laboratories). Sections are imaged with a Nikon Eclipse E200 Binocular Microscope (Nikon, Tokyo, Japan). Controls are incubated with secondary antibody only.

### Lung Microvessel Density Quantitation

The degree of pulmonary angiogenesis was evaluated by quantifying microvessel densities in lung sections immunostained with the endothelial marker FVIII, as previously described.[11,20] All stained objects were counted in a blinded manner. Vessels with thick muscular walls or larger than 100 μm in diameter were excluded. Five randomly scanned fields of three sections from each animal were investigated. The average microvessel count in each group was expressed relative to the count of the sham group as fold control values.

### Endothelial Cell Culture

Rat pulmonary microvascular endothelial cells (RPMVECs; Vec Technologies, Rensselaer, NY) were maintained and subcultured in complete media MCDB-131 (Vec Technologies) at 37°C in the presence of humidified 95% air and 5% $CO_2$. Cell passages were between 2 and 10.

### Adenoviral RPMVEC Infection and Treatments

RPMVECs were plated in 6-well plates and allowed to reach 80% confluence. Adenoviral-CMV-$ET_B$ receptor constructs (1000 viral particle per cell) were added to cells for 24 to 48 hours to recapitulate *in vivo* alterations of HPS, as previously described.[19] Adenovirus-cytomegalovirus–green fluorescent protein (AdCMV-GFP) constructs were used as control. After transfection, cells were stimulated with 1 to approximately 50 nmol/L ET-1 (Bachem Americas, Inc, Torrance,

CA) in the absence or presence of a selective $ET_B$ receptor antagonist (BQ788) and specific inhibitors for the phospholipase C (PLC)/$InsP_3$/$Ca^{2+}$/calmodulin pathway [U73122, 2-Aminoethoxydiphenyl borate (2-APB), BAPTA acetoxymethyl ester (BAPTA-AM), and W7], mitogen-activated protein kinase (MEK)/ERK (U0126), and Akt (wortmannin) (Calbiochem). Cell and supernatant CX3CL1 expression was measured by real-time quantitative RT-PCR and enzyme-linked immunosorbent assay (ELISA). Akt and ERK phosphorylation was assessed by using Western blot analysis.

### Measurement of Cell Culture Medium CX3CL1 Levels

RPMVEC supernatant CX3CL1 levels were measured with a commercial ELISA kit (Bio-Rad Laboratories, Hercules, CA), according to the manufacturer's instructions.

### RNA Extraction and Quantitative Real-Time RT-PCR

Total RNA from lung or RPMVECs was extracted with TRIzol (Invitrogen, Carlsbad, CA) reagent, according to the manufacturer's instructions, and treated with RNase-free DNase I (Invitrogen), following the manufacturer's protocol. cDNA was prepared using The High Capacity cDNA Reverse Transcription kit (Life Technologies, Grand Island, NY). Real-time PCR analysis was performed using the StepOnePlus Real-Time PCR System and TaqMan Gene Expression Master Mix (Life Technologies), according to the manufacturer's recommendations. TaqMan Gene Expression Assays for rat CX3CL1 and CX3CR1 were from Life Technologies. Expression levels were normalized to expression of 18S rRNA.

### Western Blot Analysis

Equal amounts of proteins from the lung or cell lysates, obtained as previously described, were fractionated on Criterion Tris-HCl Gel (4% to 20%; Bio-Rad Laboratories) and transferred to a polyvinylidene difluoride membrane (EMD Millipore Corporation, Billerica, MA). Incubation with primary antibodies against ED1, Akt, p-Akt (Ser473), ERK, and p-ERK (Thr202/Tyr204; Cell Signaling Technology, Inc, Danvers, MA) was followed by addition of horseradish peroxidase–conjugated secondary antibodies and detection with enhanced chemiluminescence substrate Pico-West luminol reagent (Thermo Scientific Pierce, Rockford, IL). The density of autoradiographic signals was assessed with a ScanMaker i900 scanner (Microtek Lab, Carson, CA) and quantitated with ImageJ software version 1.47 (NIH, Bethesda, MD).

### Endothelial Tube Formation Assay

ET-1 stimulation of endothelial cell tube formation (*in vitro* angiogenesis) was assessed by culturing RPMVECs on growth factor–reduced Matrigel (BD Biosciences, Franklin Lakes, NJ). RPMVECs were transfected with AdCMV-$ET_B$ receptor constructs (1000 viral particle per cell) for 40 hours, as previously described. A total of $4 \times 10^4$ transfected RPMVECs per well were added to a 48-well plate coated with Matrigel and incubated (Eagle's basal medium-2 with 1.5% fetal bovine serum) for 3 to 12 hours at 37°C. ET-1 (10 nmol/L) was administered in the presence or absence of a selective $ET_B$ receptor antagonist (BQ788) and specific inhibitors for the PLC/$InsP_3$/$Ca^{2+}$/calmodulin pathway (U73122, 2-APB, BAPTA-AM, W7), MEK/ERK (U0126), Akt (wortmannin), and an anti-CX3CR1 neutralizing antibody (Torrey Pines Biolabs, East Orange, NJ). Five random fields per well were captured using a Nikon Eclipse E200 Binocular Microscope. Endothelial tubular structures were skeletonized, and total tube length was quantified in a blinded manner and expressed as fold control values.

### Statistics

Data were analyzed with the Student's *t*-test or the analysis of variance with Bonferroni correction for multiple comparisons between groups. Measurements are expressed as means ± SE. Statistical significance was designated as $P < 0.05$.

## Results

### Selective $ET_B$ Receptor Inhibition Blocks Lung Chemokine CX3CL1 Expression and Monocyte Accumulation in Experimental HPS

To evaluate the specific effects of $ET_B$ receptor blockade on lung monocyte alterations in experimental HPS, a selective $ET_B$ receptor antagonist, BQ788, was given to 1-week CBDL animals for 2 weeks, as previously described.[14] Lung mRNA levels of CX3CL1 and its receptor, CX3CR1, were measured by real-time RT-PCR. Monocyte accumulation in the lung vasculature was assessed by ED1 (CD68, a pan-monocyte marker) immunohistochemistry (IHC) and protein levels. Relative to sham animals, CBDL animals developed significant portal hypertension, reflected by elevated portal venous pressure and spleen weight and a widened $AaPO_2$, indicating the development of HPS. BQ788 administration to CBDL animals improved gas exchange abnormalities without influencing portal hypertension (Supplemental Figure S1), similar to prior reports.[14]

CBDL also resulted in a marked increase in pulmonary CX3CL1 expression and endothelial staining, which was accompanied by vascular monocyte infiltration, consistent with our prior findings.[20] These increases in lung were significantly attenuated by the blockade of the $ET_B$ receptor with BQ788 (Figure 1). CX3CR1 mRNA levels also increased in CBDL lung, reflecting the increase in monocyte numbers on the basis of ED1 IHC and protein levels. Accordingly, the decline in lung vascular monocyte

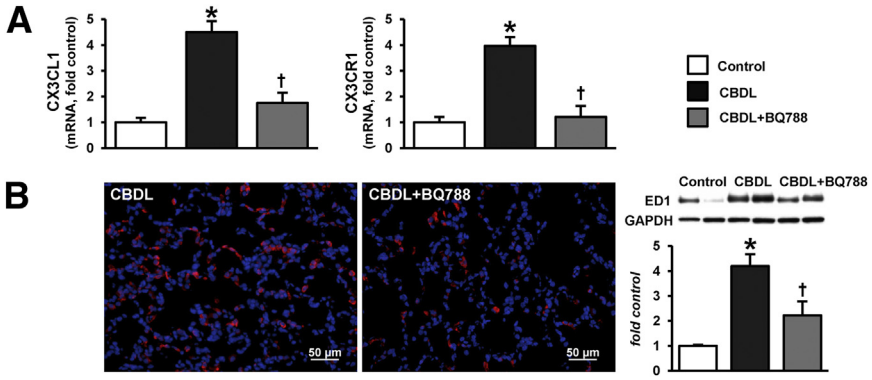


**Figure 1** Effects of $ET_B$ receptor inhibition with BQ788 on lung CX3CL1/CX3CR1 levels and monocyte accumulation after CBDL. **A:** mRNA levels for CX3CL1 and CX3CR1 in lung. **B:** Representative immunofluorescence staining for ED1 (monocyte marker, red) in lung and representative immunoblots and summary of lung ED1 protein levels. Values are expressed as means ± SEM ($n = 8$ animals for each group). $^*P < 0.05$ versus control; $^\dagger P < 0.05$ versus CBDL. Scale bar = 50 μm. GAPDH, glyceraldehyde-3-phosphate dehydrogenase.

accumulation after BQ788 administration was associated with a reduction in lung CX3CR1 (Figure 1).

To define whether monocyte infiltration and modulation by $ET_B$ receptor inhibition are selective events in the lung after CBDL, we evaluated other immune cell types in the lung and assessed liver monocyte subsets. At the light level, cells infiltrating the lung appeared to be mononuclear and stained for ED1, not ED2 (CD163, resident macrophage marker) (Figure 1A and Supplemental Figure S2). When CBDL lung (with and without BQ788 treatment) was stained for CD3 (T-cell marker) and CD45R (B-cell marker), there was no detectable accumulation, supporting a selective influx of monocytes (Supplemental Figure S3). Both infiltrated circulating monocyte and resident macrophage (Kupffer cell) subsets contribute to liver injury after CBDL.[27–29] To determine whether systemic $ET_B$ receptor blockade influences these cells, we assessed ED1 (monocyte marker) and ED2 (resident Kupffer cell marker) staining. There was a marked increase in both ED1 and ED2 staining in the liver after CBDL, which was not influenced by BQ788, supporting a lack of effect of $ET_B$ receptors on monocyte alterations in the liver (Supplemental Figure S4).

## Selective $ET_B$ Receptor Antagonist Decreases Lung Angiogenesis and Angiogenic Signaling Pathway Activation

To define whether changes in CX3CL1/CX3CR1 expression and monocyte accumulation due to $ET_B$ receptor inhibition influence activation of angiogenic pathways and angiogenesis, we assessed lung Akt and ERK activation and angiogenesis after CBDL, with or without BQ788 treatment (Figure 2). Akt and ERK phosphorylation and lung angiogenesis were significantly increased after CBDL, as previously described,[11,20] and were ameliorated by BQ788 administration.

## Effects of ET-1 on CX3CL1 Expression in Pulmonary Microvascular Endothelial Cells

To explore whether the ET-1/$ET_B$ receptor axis directly influences endothelial CX3CL1 expression, we generated $ET_B$ receptor overexpressing RPMVECs as an *in vitro* model of pulmonary microvascular alterations in experimental HPS (Supplemental Figure S5).[14,17,19,30] CX3CL1 mRNA and supernatant protein levels were quantified by real-time RT-PCR and ELISA. ET-1 administration to control RPMVECs did not alter CX3CL1 mRNA or protein production. ET-1 stimulation of $ET_B$ receptor overexpressing RPMVECs induced a significant dose- and time-dependent increase in cellular CX3CL1 mRNA production and supernatant protein levels (Figure 3A), which were blocked by $ET_B$ receptor inhibition (Figure 3B).

To define pathways involved in ET-1 stimulation of CX3CL1 in RPMVECs, we assessed activation of signaling pathways recognized either to regulate endothelial CX3CL1 production or to be activated by $ET_B$ receptor stimulation, PLC/$InsP_3$/$Ca^{2+}$/calmodulin, MEK/ERK, and Akt.[19,31–33] ET-1 administration did not influence Akt activation in either

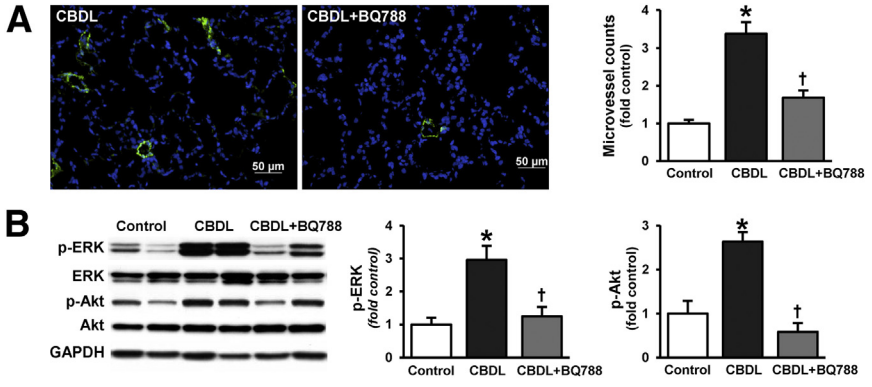


**Figure 2** Effects of $ET_B$ receptor inhibition with BQ788 on pulmonary angiogenesis and Akt and ERK phosphorylation after CBDL. **A:** Representative immunofluorescence images of lung microvessel staining (FVIII, green) and quantitation of microvessel density after CBDL. **B:** Representative immunoblots of p-Akt (Ser473) and p-ERK (Thr202/Tyr204) after CBDL and summary of protein levels for p-Akt/Akt and p-ERK/ERK. Values are expressed as means ± SEM ($n = 8$ animals for each group). $^*P < 0.05$ versus control; $^\dagger P < 0.05$ versus CBDL. Scale bar = 50 μm. GAPDH, glyceraldehyde-3-phosphate dehydrogenase.

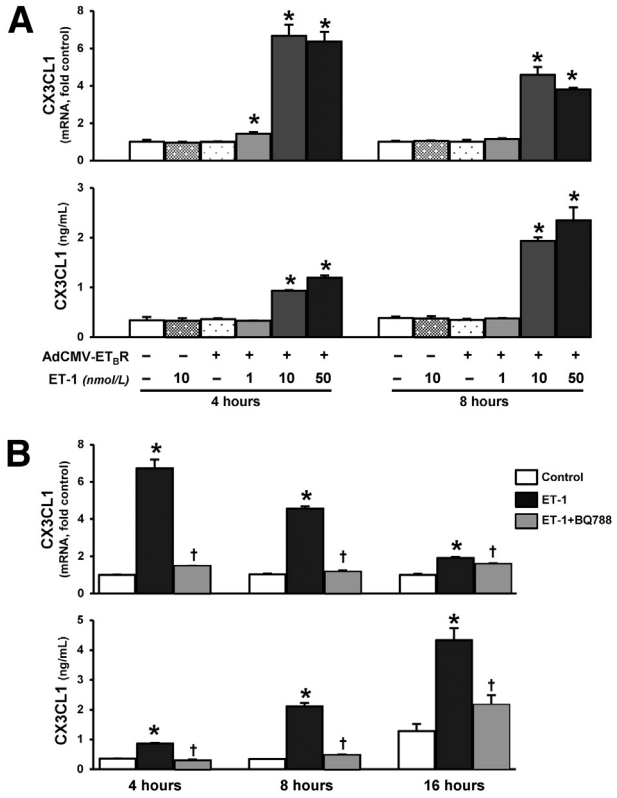


**Figure 3** Effects of ET-1 on CX3CL1 production in $ET_B$ receptor–overexpressing RPMVECs. **A:** CX3CL1 mRNA and supernatant protein levels in RPMVECs treated with 1, 10, and 50 nmol/L ET-1 for 4 and 8 hours, respectively. **B:** CX3CL1 mRNA and supernatant protein levels in 10 nmol/L ET-1–treated RPMVECs in the presence or absence of 10 μmol/L BQ788, respectively, for 4, 8, and 16 hours. Values are expressed as means ± SEM ($n = 3$ independent experiments in duplicate). $^*P < 0.05$ versus control; $^\dagger P < 0.05$ versus ET-1 treatment.

control or $ET_B$ receptor overexpressing endothelial cells, consistent with our prior *in vitro* findings (Supplemental Figure S6).[19] ET-1 stimulation of $ET_B$ receptor overexpressing cells resulted in $ET_B$ receptor–dependent ERK1/2 phosphorylation (Figure 4A and Supplemental Figure S3), which was attenuated by specific MEK inhibition (Figure 4B), but did not induce ERK activation in control cells (Supplemental Figure S6A). The activation of ERK was not altered by $Ca^{2+}$ signaling pathway inhibitors, including U73122 (PLC), 2-APB ($InsP_3$), BAPTA-AM (calcium chelator), and W7 (calmodulin), demonstrating $Ca^{2+}$-independent MEK/ERK activation (Figure 4B). Inhibition of either MEK/ERK activation or PLC/$InsP_3$/$Ca^{2+}$/calmodulin significantly attenuated ET-1–induced CX3CL1 mRNA and protein production, whereas Akt inhibition did not (Figure 5).

### Effects of ET-1 on VEGF-A Expression in Pulmonary Microvascular Endothelial Cells

VEGF-A is also established to contribute to vascular remodeling in experimental HPS.[11,20] To evaluate if ET-1 modulates expression of VEGF-A in lung endothelium, we measured VEGF-A mRNA levels after ET-1 administration in $ET_B$-overexpressing pulmonary microvascular endothelial cells. ET-1 stimulation did not influence VEGF-A expression (Supplemental Figure S7).

### Effects of ET-1 on *In Vitro* Angiogenesis in Pulmonary Microvascular Endothelial Cells

To determine whether and how ET-1 modulates endothelial cell angiogenic properties, we assessed tube formation after ET-1 stimulation of $ET_B$ receptor–overexpressing RPMVECs in the presence or absence of BQ788 (Figure 6). Relative to untreated cells, ET-1 stimulation resulted in a marked increase in tube formation expressed by relative tube length. This increase was completely inhibited by BQ788 pretreatment and was significantly inhibited by pretreatment with a neutralizing CX3CR1 antibody. Accordingly, pretreatment of endothelial cells with specific inhibitors of $Ca^{2+}$ signaling and MEK/ERK also significantly decreased ET-1–stimulated tube formation to a similar degree to CX3CR1 inhibition.

## Discussion

Our prior work has demonstrated an important role for the ET-1/$ET_B$ receptor system in the development of intrapulmonary vasodilation in experimental HPS, through the

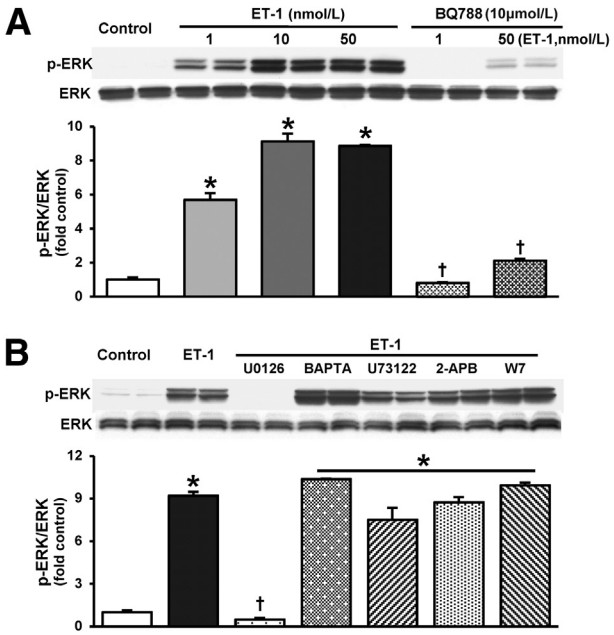


**Figure 4** Effects of ET-1 on ERK activation in $ET_B$ receptor–overexpressing RPMVECs. Representative immunoblots and graphs summarize ERK1/2 phosphorylation (Thr202/Tyr204) in RPMVECs treated with 1, 10, and 50 nmol/L ET-1 in the presence or absence of 10 μmol/L BQ788 for 5 minutes (**A**); and 10 nmol/L ET-1 in the presence or absence of 10 μmol/L MEK/ERK inhibitor U0126 and inhibitors of PLC/$InsP_3$/$Ca^{2+}$/calmodulin pathway (5 μmol/L U73122, 20 μmol/L 2-APB, 5 μmol/L BAPTA-AM, and 10 μmol/L W7, respectively) (**B**). Values are expressed as means ± SEM ($n = 3$ independent experiments in duplicate). $^*P < 0.05$ versus control; $^\dagger P < 0.05$ versus ET-1 treatment.

sequential activation of eNOS/NO signaling.[14,15,19,30] We have also shown that lung CX3CL1 expression is increased after CBDL and drives the accumulation of VEGF-A–producing monocytes and lung angiogenesis.[20] In the present study, we define that ET-1/$ET_B$ receptor activation has a novel direct effect on lung microvascular endothelial cell CX3CL1 expression, thereby linking these two pathways and the effects on the microvasculature. Specifically, we found that ET-1 stimulation of $ET_B$ receptor–overexpressing RPMVECs *in vitro* directly increased CX3CL1 expression through two independent intracellular signaling pathways, MEK/ERK and $Ca^{2+}$. Furthermore, inhibition of ET-1/$ET_B$ activation *in vivo* using a selective $ET_B$ receptor antagonist significantly reduced pulmonary CX3CL1 expression, decreased vascular monocyte accumulation, and improved angiogenesis and HPS. Finally, we found that ET-1/$ET_B$ receptor activation in $ET_B$ receptor–overexpressing RPMVECs drives tube formation *in vitro*, in part through increased CX3CL1 production. These observations directly link ET-1/$ET_B$ receptor activation and endothelial CX3CL1 production in the pathogenesis of pulmonary vascular alterations in experimental HPS.

In CBDL lung, monocyte accumulation and adhesion to the microvasculature are important pathogenic features that involve up-regulation and activation of the CX3CL1/CX3CR1 pathway.[12,20] A variety of stimuli are recognized to increase CX3CL1 mRNA and protein expression in vascular endothelial cells, including proinflammatory cytokines (lipopolysaccharide, tumor necrosis factor-α, interferon-γ, and IL-1), glucose, and resistin.[34–37] These stimuli generally signal through several intracellular pathways, including mitogen-activated protein kinases (ERK and p38), NF-κB, and STAT-1, that modulate cellular CX3CL1 expression and shedding.[38–40] Several of these pathways are also activated by ET-1,[31,33,41–44] which is up-regulated after CBDL. In addition, ET-1 acting through either the $ET_A$ or $ET_B$ receptor, has been established to increase production of other chemokines and adhesion molecules in a variety of cell types.[45–47] Therefore, we hypothesized a potential link between pulmonary microvascular ET-1/$ET_B$ receptor activation and CX3CL1 alterations in experimental HPS. Our most important finding is that ET-1, via the $ET_B$ receptor, directly induces ERK- and $Ca^{2+}$-dependent and Akt-independent CX3CL1 production in rat pulmonary microvascular endothelial cells. However, the significance of this finding is underlined by the *in vivo* observation that $ET_B$ receptor blockade using BQ788 also reduces CX3CL1 levels in lung in conjunction with improving HPS after CBDL. The finding that both mRNA levels and the secreted form of CX3CL1 are increased in ET-1–treated endothelial cells suggests that ET-1 may not only alter transcription, but could also influence cleavage or shedding from the membrane. CX3CL1 shedding occurs at the cell surface within the transmembrane domain and is attributed to specific sheddases, a disintegrin and metalloproteases 10 and 17 (known as tumor necrosis factor-α–converting enzymes).[48–50] Further studies are needed to define if and how ET-1 directly influences shedding of CX3CL1.

Our prior work has shown that ET-1/$ET_B$ receptor activation of intracellular $Ca^{2+}$ signaling stimulates eNOS activation and NO-mediated pulmonary vasodilation, independent of Akt activation after CBDL.[19] This effect on $Ca^{2+}$ pathways is influenced by the level of $ET_B$ receptor expression in the pulmonary microvasculature, which is increased in the setting of elevated shear stress.[19] Herein, we confirm that the level of $ET_B$ receptor expression in RPMVECs influences cellular responses to ET-1 and that ET-1 does not directly activate Akt *in vitro*. We do identify ET-1 activation of both $Ca^{2+}$- and ERK-dependent pathways as important intracellular modulators of CX3CL1 expression. Lung Akt activation is increased *in vivo* during angiogenesis after CBDL and is inhibited by $ET_B$ receptor, CX3CR1, or VEGF-A blockade.[11,20] These findings are consistent with the concept that ET-1 effects on Akt in the pulmonary endothelium *in vivo* are mediated indirectly, through up-regulation of CX3CL1 autocrine/paracrine

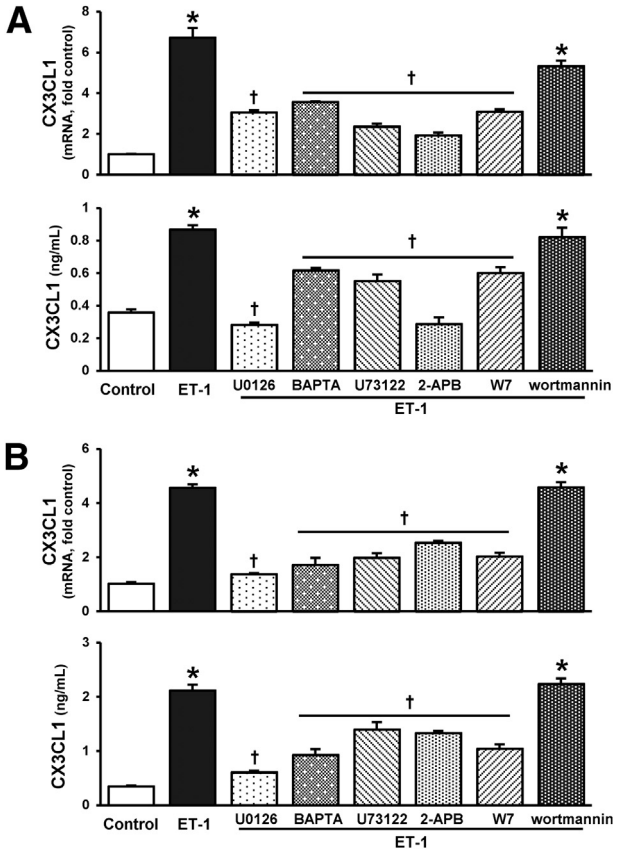


**Figure 5** Effects of $Ca^{2+}$ and MEK/ERK pathway inhibition on ET-1–stimulated CX3CL1 production in $ET_B$ receptor–overexpressing RPMVECs. CX3CL1 mRNA and supernatant protein levels in RPMVECs treated with 10 nmol/L ET-1 in the presence or absence of inhibitors of MEK/ERK (10 μmol/L U0126), PLC/$InsP_3$/$Ca^{2+}$/calmodulin pathway (5 μmol/L U73122, 20 μmol/L 2-APB, 5 μmol/L BAPTA-AM, and 10 μmol/L W7), and Akt (0.5 μmol/L wortmannin) for 4 (**A**) and 8 (**B**) hours. Values are expressed as means ± SEM ($n = 3$ independent experiments in duplicate). $^*P < 0.05$ versus control; $^\dagger P < 0.05$ versus ET-1 treatment.

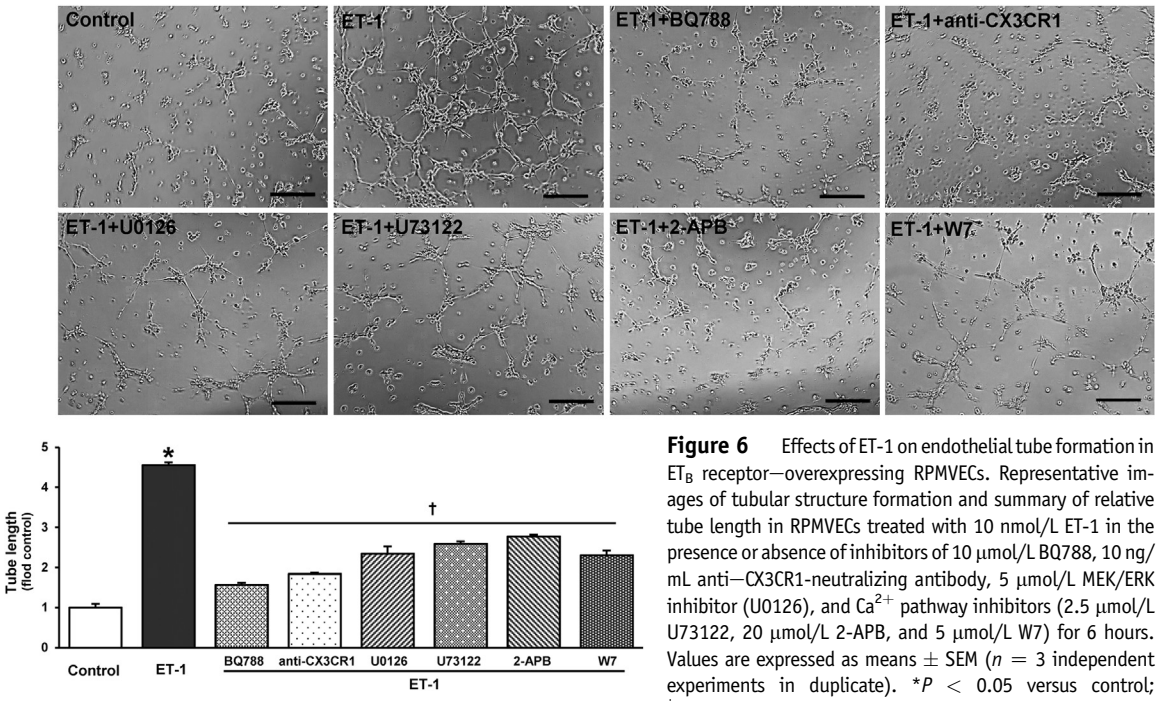


**Figure 6** Effects of ET-1 on endothelial tube formation in $ET_B$ receptor—overexpressing RPMVECs. Representative images of tubular structure formation and summary of relative tube length in RPMVECs treated with 10 nmol/L ET-1 in the presence or absence of inhibitors of 10 μmol/L BQ788, 10 ng/mL anti—CX3CR1-neutralizing antibody, 5 μmol/L MEK/ERK inhibitor (U0126), and $Ca^{2+}$ pathway inhibitors (2.5 μmol/L U73122, 20 μmol/L 2-APB, and 5 μmol/L W7) for 6 hours. Values are expressed as means ± SEM ($n = 3$ independent experiments in duplicate). $^*P < 0.05$ versus control; $^{\dagger}P < 0.05$ versus ET-1 treatment. Scale bar = 200 μm.

signaling and/or VEGF-A produced by adherent intravascular monocytes; each of these events activates Akt and is decreased by $ET_B$ receptor inhibition. These findings support that ET-1 initiates a cascade of alterations in the pulmonary microvasculature in the setting of increased pulmonary endothelial $ET_B$ receptor expression after CBDL, which results in activation of multiple signaling pathways in endothelial cells relevant to monocyte adherence and angiogenesis.

The *in vitro* endothelial cell tube formation assays are also consistent with direct and indirect effects of ET-1 on angiogenesis in the pulmonary microvascular endothelium in the setting of $ET_B$ receptor overexpression. The finding that $ET_B$ receptor inhibition blocks ET-1 effects on RPMVEC tubular structure formation is consistent with prior findings that ET-1 directly induces endothelial cell proliferation, migration, and angiogenic morphological characteristics[18,51,52] and with the *in vivo* studies in which $ET_B$ receptor inhibition decreased angiogenesis. These effects are likely mediated through ERK and $Ca^{2+}$ signaling pathways.[53,54] Our observation herein that blockade of CX3CR1 also inhibits ET-1—driven tubular structure formation supports that CX3CL1 production by ET-1 results in autocrine effects on endothelial cell angiogenic potential. These findings occur in parallel to the established *in vivo* effects of CX3CL1 on monocyte adherence after CBDL. These results support that ET-1 modulation of endothelial CX3CL1 production is one key indirect pathway for influencing endothelial angiogenesis and monocyte adherence. Future studies need to address the precise interaction between ET-1 and CX3CL1 in pulmonary angiogenesis using genetic approaches to selectively ablate endothelial CX3CL1 expression.

In endothelial cells from other tissues, ET-1 has been reported to increase expression of members of the VEGF family (VEGF-A and VEGF-C), indirectly regulating cell proliferation and angiogenic responses.[51,52,55] In contrast, our *in vitro* studies herein demonstrate that ET-1 does not increase VEGF-A expression in RPMVECs over a 4- to 18-hour time frame. This finding suggests that endothelial production of VEGF in response to ET-1 may vary by tissue and is consistent with the lack of effect of ET-1 on Akt activation in RPMVECs. We have identified intravascular monocytes recruited into the lung after CBDL as a major source of VEGF-A production, supporting a paracrine mechanism for monocytes in the development of lung angiogenesis in experimental HPS.[11,20] However, a degree of VEGF-A staining has also been detected in the lung microvasculature once experimental HPS has developed,

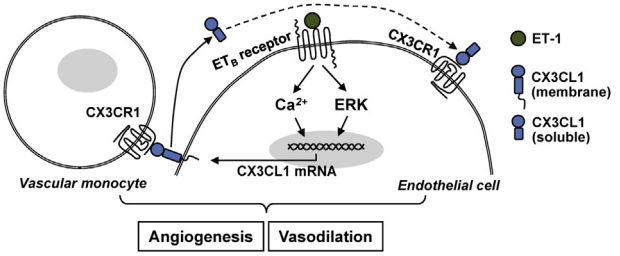


**Figure 7** Working model of the ET-1/$ET_B$ receptor axis and the pulmonary vascular endothelial CX3CL1/CX3CR1 pathway in the development of experimental HPS.

suggesting that additional mediators and cell types may modulate VEGF-A production in pulmonary microvasculature *in vivo* after CBDL.

We have identified a novel synergistic interplay between ET-1 acting through the $ET_B$ receptor and increased CX3CL1 expression in RPMVECs that contributes to altered angiogenic potential and influences monocyte adhesion and the clinical expression of experimental HPS (Figure 7). These effects occur through $Ca^{2+}$- and MEK/ERK-mediated intracellular signaling pathways and are supported by *in vivo* findings showing that $ET_B$ receptor blockade inhibits lung angiogenesis and monocyte accumulation by down-regulation of CX3CL1/CX3CR1 signaling. This direct link between hepatic ET-1 production and pulmonary vascular alterations in experimental HPS may have relevance to human disease on the basis of the recent finding that hepatic venous ET-1 levels are elevated in patients with pulmonary microvascular dilation relative to those without pulmonary microvascular alterations.[56] Understanding the cellular mechanisms of experimental HPS may provide important insight into understanding and treating human disease.

## Supplemental Data

Supplemental material for this article can be found at *http://dx.doi.org/10.1016/j.ajpath.2014.02.027*.

## References


1. Cahill PA, Redmond EM, Sitzmann JV: Endothelial dysfunction in cirrhosis and portal hypertension. Pharmacol Ther 2001, 89:273–293
2. Lee JS, Semela D, Iredale J, Shah VH: Sinusoidal remodeling and angiogenesis: a new function for the liver-specific pericyte? Hepatology 2007, 45:817–825
3. Rodriguez-Roisin R, Krowka MJ: Hepatopulmonary syndrome: a liver-induced lung vascular disorder. N Engl J Med 2008, 358: 2378–2387
4. Rodriguez-Roisin R, Krowka MJ, Herve P, Fallon MB; ERS Task Force Pulmonary-Hepatic Vascular Disorders Scientific Committee ERS Task Force PHD Scientific Committee: Pulmonary-hepatic vascular disorders (PHD). Eur Respir J 2004, 24:861–880
5. Schenk P, Schoniger-Hekele M, Fuhrmann V, Madl C, Silberhumer G, Muller C: Prognostic significance of the hepatopulmonary syndrome in patients with cirrhosis. Gastroenterology 2003, 125:1042–1052
6. Fallon MB, Krowka MJ, Brown RS, Trotter JF, Zacks S, Roberts KE, Shah VH, Kaplowitz N, Forman L, Wille K, Kawut SM: Impact of hepatopulmonary syndrome on quality of life and survival in liver transplant candidates. Gastroenterology 2008, 135:1168–1175
7. Sztrymf B, Rabiller A, Nunes H, Savale L, Lebrec D, LePape A, de Montpreville V, Mazmanian M, Humbert M, Herve P: Prevention of hepatopulmonary syndrome by pentoxifylline in cirrhotic rats. Eur Respir J 2004, 23:752–758
8. Fallon MB, Abrams GA, McGrath JW, Hou Z, Luo B: Common bile duct ligation in the rat: a model of intrapulmonary vasodilatation and hepatopulmonary syndrome. Am J Physiol 1997, 272: G779–G784
9. Luo B, Tang L, Wang Z, Zhang J, Ling Y, Feng W, Sun JZ, Stockard CR, Frost AR, Chen YF, Grizzle WE, Fallon MB: Cholangiocyte endothelin 1 and transforming growth factor beta1 production in rat experimental hepatopulmonary syndrome. Gastroenterology 2005, 129:682–695
10. Thenappan T, Goel A, Marsboom G, Fang YH, Toth PT, Zhang HJ, Kajimoto H, Hong Z, Paul J, Wietholt C, Pogoriler J, Piao L, Rehman J, Archer SL: A central role for CD68(+) macrophages in hepatopulmonary syndrome: reversal by macrophage depletion. Am J Respir Crit Care Med 2011, 183:1080–1091
11. Zhang J, Luo B, Tang L, Wang Y, Stockard CR, Kadish I, Van Groen T, Grizzle WE, Ponnazhagan S, Fallon MB: Pulmonary angiogenesis in a rat model of hepatopulmonary syndrome. Gastroenterology 2009, 136:1070–1080
12. Zhang J, Ling Y, Luo B, Tang L, Stockard C, Grizzle WE, Fallon MB: Analysis of pulmonary heme oxygenase-1 and nitric oxide synthase alterations in experimental hepatopulmonary syndrome. Gastroenterology 2003, 125:1441–1451
13. Nunes H, Lebrec D, Mazmanian M, Capron F, Heller J, Tazi KA, Zerbib E, Dulmet E, Moreau R, Dinh-Xuan AT, Simonneau G, Herve P: Role of nitric oxide in hepatopulmonary syndrome in cirrhotic rats. Am J Respir Crit Care Med 2001, 164:879–885
14. Ling Y, Zhang J, Luo B, Song D, Liu L, Tang L, Stockard C, Grizzle W, Ku D, Fallon MB: The role of endothelin-1 and the endothelin B receptor in the pathogenesis of experimental hepatopulmonary syndrome. Hepatology 2004, 39:1593–1602
15. Fallon MB, Abrams GA, Luo B, Hou Z, Dai J, Ku DD: The role of endothelial nitric oxide synthase in the pathogenesis of a rat model of hepatopulmonary syndrome. Gastroenterology 1997, 113:606–614
16. Liu L, Zhang M, Luo B, Abrams GA, Fallon MB: Biliary cyst fluid from common bile duct ligated rats stimulates eNOS in pulmonary artery endothelial cells: a potential role in hepatopulmonary syndrome. Hepatology 2001, 33:722–727
17. Luo B, Liu L, Tang L, Zhang J, Stockard C, Grizzle W, Fallon M: Increased pulmonary vascular endothelin B receptor expression and responsiveness to endothelin-1 in cirrhotic and portal hypertensive rats: a potential mechanism in experimental hepatopulmonary syndrome. J Hepatol 2003, 38:556–563
18. Zhang M, Luo B, Chen SJ, Abrams GA, Fallon MB: Endothelin-1 stimulation of endothelial nitric oxide synthase in the pathogenesis of hepatopulmonary syndrome. Am J Physiol 1999, 277:G944–G952
19. Tang L, Luo B, Patel RP, Ling Y, Zhang J, Fallon MB: Modulation of pulmonary endothelial endothelin B receptor expression and signaling: implications for experimental hepatopulmonary syndrome. Am J Physiol Lung Cell Mol Physiol 2007, 292:L1467–L1472
20. Zhang J, Yang W, Luo B, Hu B, Maheshwari A, Fallon MB: The role of CX3CL1/CX3CR1 in pulmonary angiogenesis and intravascular monocyte accumulation in rat experimental hepatopulmonary syndrome. J Hepatol 2012, 57:752–758
21. Bazan JF, Bacon KB, Hardiman G, Wang W, Soo K, Rossi D, Greaves DR, Zlotnik A, Schall TJ: A new class of membrane-bound chemokine with a CX3C motif. Nature 1997, 385:640–644
22. Imai T, Hieshima K, Haskell C, Baba M, Nagira M, Nishimura M, Kakizaki M, Takagi S, Nomiyama H, Schall TJ, Yoshie O: Identification and molecular characterization of fractalkine receptor CX3CR1, which mediates both leukocyte migration and adhesion. Cell 1997, 91:521–530
23. Teupser D, Pavlides S, Tan M, Gutierrez-Ramos JC, Kolbeck R, Breslow JL: Major reduction of atherosclerosis in fractalkine (CX3CL1)-deficient mice is at the brachiocephalic artery, not the aortic root. Proc Natl Acad Sci U S A 2004, 101:17795–17800
24. Volin MV, Huynh N, Klosowska K, Reyes RD, Woods JM: Fractalkine-induced endothelial cell migration requires MAP kinase signaling. Pathobiology 2010, 77:7–16
25. Lee SJ, Namkoong S, Kim YM, Kim CK, Lee H, Ha KS, Chung HT, Kwon YG, Kim YM: Fractalkine stimulates angiogenesis by activating the Raf-1/MEK/ERK- and PI3K/Akt/eNOS-dependent signal pathways. Am J Physiol Heart Circ Physiol 2006, 291: H2836–H2846

26. Luo B, Liu L, Tang L, Zhang J, Ling Y, Fallon MB: ET-1 and TNF-alpha in HPS: analysis in prehepatic portal hypertension and biliary and nonbiliary cirrhosis in rats. Am J Physiol Gastrointest Liver Physiol 2004, 286:G294–G303
27. Karlmark K, Weiskirchen R, Zimmermann H, Gassler N, Ginhoux F, Weber C, Merad M, Luedde T, Trautwein C, Tacke F: Hepatic recruitment of the inflammatory Gr1+ monocyte subset upon liver injury promotes hepatic fibrosis. Hepatology 2009, 50:261–274
28. Ramachandran P, Iredale JP: Macrophages: central regulators of hepatic fibrogenesis and fibrosis resolution. J Hepatol 2012, 56:1417–1419
29. Wynn TA, Barron L: Macrophages: master regulators of inflammation and fibrosis. Semin Liver Dis 2010, 30:245–257
30. Liu L, Luo B, Wang Z, Abrams GA, Fallon MB: Endothelin-1 stimulates eNOS expression and activity in rat pulmonary microvascular endothelial cells. Hepatology 2001, 34:184A
31. Chen QW, Edvinsson L, Xu CB: Role of ERK/MAPK in endothelin receptor signaling in human aortic smooth muscle cells. BMC Cell Biol 2009, 10:52
32. Creighton JR, Masada N, Cooper DM, Stevens T: Coordinate regulation of membrane cAMP by Ca2+-inhibited adenylyl cyclase and phosphodiesterase activities. Am J Physiol Lung Cell Mol Physiol 2003, 284:L100–L107
33. Deliu E, Brailoiu GC, Mallilankaraman K, Wang H, Madesh M, Undieh AS, Koch WJ, Brailoiu E: Intracellular endothelin type B receptor-driven Ca2+ signal elicits nitric oxide production in endothelial cells. J Biol Chem 2012, 287:41023–41031
34. Imaizumi T, Yoshida H, Satoh K: Regulation of CX3CL1/fractalkine expression in endothelial cells. J Atheroscler Thromb 2004, 11: 15–21
35. Matsumiya T, Ota K, Imaizumi T, Yoshida H, Kimura H, Satoh K: Characterization of synergistic induction of CX3CL1/fractalkine by TNF-alpha and IFN-gamma in vascular endothelial cells: an essential role for TNF-alpha in post-transcriptional regulation of CX3CL1. J Immunol 2010, 184:4205–4214
36. Manduteanu I, Dragomir E, Calin M, Pirvulescu M, Gan AM, Stan D, Simionescu M: Resistin up-regulates fractalkine expression in human endothelial cells: lack of additive effect with TNF-alpha. Biochem Biophys Res Commun 2009, 381:96–101
37. Manduteanu I, Pirvulescu M, Gan AM, Stan D, Simion V, Dragomir E, Calin M, Manea A, Simionescu M: Similar effects of resistin and high glucose on P-selectin and fractalkine expression and monocyte adhesion in human endothelial cells. Biochem Biophys Res Commun 2010, 391:1443–1448
38. Uchida M, Ito T, Nakamura T, Igarashi H, Oono T, Fujimori N, Kawabe K, Suzuki K, Jensen RT, Takayanagi R: ERK pathway and sheddases play an essential role in ethanol-induced CX3CL1 release in pancreatic stellate cells. Lab Invest 2013, 93:41–53
39. Lee AS, Jung YJ, Kim DH, Lee TH, Kang KP, Lee S, Lee NH, Sung MJ, Kwon DY, Park SK, Kim W: Epigallocatechin-3-O-gallate decreases tumor necrosis factor-α–induced fractalkine expression in endothelial cells by suppressing NF-κB. Cell Physiol Biochem 2009, 24:503–510
40. Isozaki T, Otsuka K, Sato M, Takahashi R, Wakabayashi K, Yajima N, Miwa Y, Kasama T: Synergistic induction of CX3CL1 by interleukin-1beta and interferon-gamma in human lung fibroblasts: involvement of signal transducer and activator of transcription 1 signaling pathways. Transl Res 2011, 157:64–70
41. Cramer H, Schmenger K, Heinrich K, Horstmeyer A, Boning H, Breit A, Piiper A, Lundstrom K, Muller-Esterl W, Schroeder C: Coupling of endothelin receptors to the ERK/MAP kinase pathway: roles of palmitoylation and G(alpha)q. Eur J Biochem 2001, 268: 5449–5459
42. Kulasekaran P, Scavone CA, Rogers DS, Arenberg DA, Thannickal VJ, Horowitz JC: Endothelin-1 and transforming growth factor-beta1 independently induce fibroblast resistance to apoptosis via AKT activation. Am J Respir Cell Mol Biol 2009, 41:484–493
43. Gerstung M, Roth T, Dienes HP, Licht C, Fries JW: Endothelin-1 induces NF-kappaB via two independent pathways in human renal tubular epithelial cells. Am J Nephrol 2007, 27:294–300
44. McWhinnie R, Pechkovsky DV, Zhou D, Lane D, Halayko AJ, Knight DA, Bai TR: Endothelin-1 induces hypertrophy and inhibits apoptosis in human airway smooth muscle cells. Am J Physiol Lung Cell Mol Physiol 2007, 292:L278–L286
45. Chen P, Shibata M, Zidovetzki R, Fisher M, Zlokovic BV, Hofman FM: Endothelin-1 and monocyte chemoattractant protein-1 modulation in ischemia and human brain-derived endothelial cell cultures. J Neuroimmunol 2001, 116:62–73
46. Simonson MS, Ismail-Beigi F: Endothelin-1 increases collagen accumulation in renal mesangial cells by stimulating a chemokine and cytokine autocrine signaling loop. J Biol Chem 2011, 286: 11003–11008
47. Li L, Chu Y, Fink GD, Engelhardt JF, Heistad DD, Chen AF: Endothelin-1 stimulates arterial VCAM-1 expression via NADPH oxidase-derived superoxide in mineralocorticoid hypertension. Hypertension 2003, 42:997–1003
48. Garton KJ, Gough PJ, Blobel CP, Murphy G, Greaves DR, Dempsey PJ, Raines EW: Tumor necrosis factor-alpha-converting enzyme (ADAM17) mediates the cleavage and shedding of fractalkine (CX3CL1). J Biol Chem 2001, 276:37993–38001
49. Hurst LA, Bunning RA, Sharrack B, Woodroofe MN: siRNA knockdown of ADAM-10, but not ADAM-17, significantly reduces fractalkine shedding following pro-inflammatory cytokine treatment in a human adult brain endothelial cell line. Neurosci Lett 2012, 521: 52–56
50. Hundhausen C, Misztela D, Berkhout TA, Broadway N, Saftig P, Reiss K, Hartmann D, Fahrenholz F, Postina R, Matthews V, Kallen KJ, Rose-John S, Ludwig A: The disintegrin-like metalloproteinase ADAM10 is involved in constitutive cleavage of CX3CL1 (fractalkine) and regulates CX3CL1-mediated cell-cell adhesion. Blood 2003, 102:1186–1195
51. Spinella F, Garrafa E, Di Castro V, Rosano L, Nicotra MR, Caruso A, Natali PG, Bagnato A: Endothelin-1 stimulates lymphatic endothelial cells and lymphatic vessels to grow and invade. Cancer Res 2009, 69: 2669–2676
52. Salani D, Taraboletti G, Rosano L, Di Castro V, Borsotti P, Giavazzi R, Bagnato A: Endothelin-1 induces an angiogenic phenotype in cultured endothelial cells and stimulates neovascularization in vivo. Am J Pathol 2000, 157:1703–1711
53. Chim SM, Qin A, Tickner J, Pavlos N, Davey T, Wang H, Guo Y, Zheng MH, Xu J: EGFL6 promotes endothelial cell migration and angiogenesis through the activation of extracellular signal-regulated kinase. J Biol Chem 2011, 286:22035–22046
54. Jung HJ, Kim JH, Shim JS, Kwon HJ: A novel Ca2+/calmodulin antagonist HBC inhibits angiogenesis and down-regulates hypoxia-inducible factor. J Biol Chem 2010, 285:25867–25874
55. Garrafa E, Caprara V, Di Castro V, Rosano L, Bagnato A, Spinella F: Endothelin-1 cooperates with hypoxia to induce vascular-like structures through vascular endothelial growth factor-C, -D and -A in lymphatic endothelial cells. Life Sci 2012, 91:638–643
56. Koch DG, Bogatkevich G, Ramshesh V, Lemasters JJ, Uflacker R, Reuben A: Elevated levels of endothelin-1 in hepatic venous blood are associated with intrapulmonary vasodilatation in humans. Dig Dis Sci 2012, 57:516–523